

DOI: 10.13208/j.electrochem.131227

Cite this: *J. Electrochem.* **2014**, 20(5): 486-492

Artical ID:1006-3471(2014)05-0486-07

Http://electrochem.xmu.edu.cn

Preparation and Electrochemical Behavior of PbO/GN/AC

GAO Yun-fang*, WANG Yan-ping, YAO Qiu-shi, WANG Fu-hua,
REN Dong-lei, XU Xin

(State Key Laboratory Breeding Base of Green Chemistry-Synthesis Technology, College of Chemical
Engineering, Zhejiang University of Technology, Hangzhou 310032, China)

Abstract: The lead oxide/graphene/activated carbon (PbO/GN/AC) composite materials were prepared by impregnating commercial activated carbon and graphene in saturated lead nitrate solution followed by calcination. The structures and morphologies of the composite were characterized by X-ray diffraction (XRD), scanning electron microscopy (SEM) and energy dispersive spectroscopy (EDS). The results show that PbO crystals (about 200 nm) were dispersed uniformly on the surface of activated carbon and graphene. Electrochemical data indicate that the composite exhibited good electrochemical performances. The PbO/GN/AC composite possessed the higher over-potential of hydrogen evolution and the high specific capacitance of $312.6 \text{ F} \cdot \text{g}^{-1}$, while the internal resistance was 1.56Ω . The composite electrode also displayed excellent cycling stability, retaining over 92.6% of its initial charge after 6000 cycles. The ultra-battery with 5% (by mass) PbO/GN/AC being added to the negative paste had a cycle life approximately 3.5 times longer than conventional lead-acid batteries.

Key words: activated carbon; PbO; graphene; hydrogen evolution; supercapacitor

CLC Number: TM912.1

Document Code: A

Due to a relatively simple, low cost and mature technology, lead-acid batteries (LABs) are still the best choice for many medium and large-scale energy-storage applications^[1]. However, low current density, relatively low specific capacitance and short service lifetime eventually limit their wider application in hybrid electric vehicles. In order to resolve these problems, CSIRO (Commonwealth Scientific and Industrial Research Organisation) Energy Technology has developed an advanced ultra-battery, which combines supercapacitor and lead-acid batteries in one unit cell^[2]. Both of the two different storage mechanisms of the electric double layer capacitance (EDLC) and faradic capacity are existed in the supercapacitor system. During the high-rate charging and discharging processes, the capacitor acts as a buffer to enhance the power and lifespan of the lead-acid

battery. Also, it can lose and obtain charge rapidly when the vehicle accelerates and brakes^[3-5].

Carbon based composite materials are used as an electrode material for EDLC supercapacitors where conducting polymers or metal oxide based materials are used as a pseudocapacitor^[6]. Activated carbon based supercapacitor has been used widely due to its low cost, abundant availability, and high surface area^[7]. Graphene, which possesses unique nanostructure and has excellent electronic conductivity, may be the ideal conductive additive for hybrid nanostructured electrode and can be considered as promising nanoscale building blocks of new composites^[8-10]. In this paper, when the GN and AC were added into the lead-acid battery, the capacity and rate performance of lead-acid battery were improved by means of enhancing conductivity, capacitive effect, and dispersion of

Received: 2013-12-27, Revised: 2014-04-22 *Corresponding author, Tel: (86) 13396581232, E-mail: gaoyf@zjut.edu.cn

The research work was supported by National Key Technology Research and Development Program of the Ministry of Science and Technology of China (No. 2014BAC03B03).

the lead sulfate. Nevertheless, the introduction of the carbon materials also introduces some problems, namely, a) a potential mismatch between the capacitor electrode and the negative plate of lead-acid batteries^[2]; b) an early evolution of hydrogen. In this article, the PbO/GN/AC composite with high over-potential of hydrogen evolution and high specific capacitance were synthesized and characterized, and the electrochemical performances were examined.

1 Experimental

1.1 Preparation of PbO/GN/AC Composite and Electrodes

The PbO/GN/AC composite can be easily synthesized as follows. Firstly, 2 g GN was dispersed in 100 mL saturated lead nitrate solution by ultrasonication for 2 h then added 4 g AC. Secondly, the mixture was filtered after using ultrasonication for 1 h and continuous stirring for 12 h at room temperature. Thirdly, the filter cake was immersed into 22% (by mass) ammonium hydroxide solution with stirring for 3 h. Finally, the solid was filtered and washed several times, and calcined at 500 °C for 3 h in a vacuum oven. The electrode was prepared by dispersing 90% (by mass) active materials and 10% (by mass) polyvinylidene fluoride (PVDF) in 1-methyl-2-pyrrolidone (NMP) to ensure the homogeneity, the slurry was then pressed onto the current collector at 5 MPa for 3 min. Finally, the electrode assembly was dried under vacuum for 12 h at 120 °C. A (1 × 1) cm titanium plate was used as a current collector. Using the same method, graphene or activated carbon electrodes were obtained.

1.2 Characterization

Morphological and microstructural investigations of the PbO/GN/AC composite were carried out using scanning electron microscope (SEM, Hitachi S-4800) and powder X-ray diffraction (XRD, PANalytical, X'Pert Pro), respectively. The energy dispersive spectrometer (EDS) was used to examine the distribution of elements on the surface.

1.3 Electrochemical Measurements

The electrochemical measurements were carried out on CHI660D electrochemical workstation at room temperature in 1.28 g·mL⁻¹ H₂SO₄ solution. The prepared electrode, platinum foil, and Hg/Hg₂SO₄

electrode were used as the working, counter, and reference electrodes, respectively. The PbO/GN/AC composite was added to the negative paste during paste mixing, in concentrations with 5.0% (by mass) versus the lead oxide. The test cells comprise one negative and two positive plates. The cells are subjected to a simplified HEV cycling test. First, the cells are discharged to 60% state of charge, and then followed by the schedule: charge at 2C rate for 60 s, rest for 10 s, discharge at 2C rate for 60 s, rest for 10 s. Cycling is stopped when the end-of-discharge voltage drops down to 1.65 V. The measurements were carried out at 25 °C.

2 Results and Discussion

2.1 Characterizations

Fig. 1 shows the XRD patterns of GN, AC and PbO/GN/AC composite. The XRD spectrum of GN shows a peak at 26.4° corresponding to reflection from (002) plane of hexagonal graphite (JCPDS Card No. 75-0444). The X-ray diffraction profile of the activated carbons has two very broad peaks. Differences in the 2θ value can be attributed to the structural differences of GN and AC, since the activated carbons have a predominantly amorphous structure, whereas the graphene layers have planar structure. For the PbO/GN/AC composite, the peaks marked with an asterisk correspond to characteristic diffraction peaks from PbO particles (JCPDS Card No. 72-0094). The graphene peak at 2θ = 26.4° overlapped with the peak from PbO. This demonstrates the existence of PbO in the composite.

SEM images of the composite are shown in Fig. 2A, 2B and 2C, from which it can be clearly observed that the GN coats closely onto the surface of activated carbon. The particles have grown successfully on a continuous GN network. Evidently, white particles show a tendency to have strong interaction with graphene. No obvious aggregations of the particles are observed in the composite. Additionally, Graphene layers interact with each other to form an open pore system, through which electrolyte ions easily access the surface of graphene to form the electric double layer. The experimental process and XRD reveal that white particles are PbO, which are crystalline in nature with an average size of 100 ~ 200

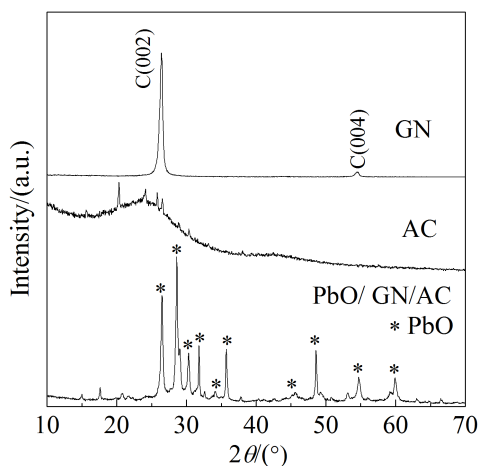


Fig. 1 XRD patterns of GN, AC and the PbO/GN/AC composite

nm. Fig. 2D is the EDS and the analysis results of corresponding element (inset of Fig. 2D) of the composite. In the selected area, the mass fractions of C and Pb in the sample are 77.54% and 16.94%, respectively. Moreover, from the elements listed in the table, it can be inferred that the composite contain mainly PbO and C, which is consistent with the XRD analysis.

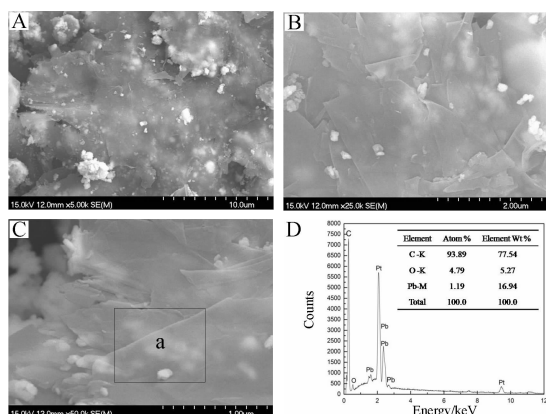


Fig. 2 SEM images (A-C) and EDS spectrum (D) of PbO/GN/AC composite

Fig. 3 shows the N_2 adsorption-desorption isotherms of GN, AC and PbO/GN/AC composite. As can be seen in Fig. 3, the data for these samples are almost the same. The BET surface areas, pore volumes, and average pore sizes of all samples are shown in Tab. 1. The BET surface areas of GN, AC and PbO/GN/AC are $560 \text{ m}^2 \cdot \text{g}^{-1}$, $1200 \text{ m}^2 \cdot \text{g}^{-1}$ and 931

$\text{m}^2 \cdot \text{g}^{-1}$, respectively. The BET surface areas of all three samples are lower than the theoretical limit ($2630 \text{ m}^2 \cdot \text{g}^{-1}$) of graphene. Furthermore, the BET surface areas and pore volumes of the obtained PbO/GN/AC composite are between those of GN and AC. The reason should be that the specific surface area of the Pb/PbO is low.

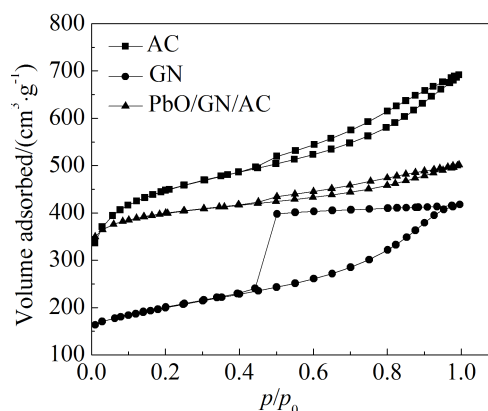


Fig. 3 Nitrogen adsorption-desorption isotherms of GN, AC and PbO/GN/AC

Tab. 1 BET surface areas, pore volumes, and average pore sizes of GN, AC and PbO/GN/AC

Sample	BET surface area/($\text{m}^2 \cdot \text{g}^{-1}$)	Pore volume/($\text{cm}^3 \cdot \text{g}^{-1}$)	Average pore size/nm
GN	560	1.626	2.5
AC	1200	0.889	4.2
PbO/GN/AC	931	0.379	5.1

2.2 Electrochemical Performance

Fig. 4 shows the linear sweep voltammograms of AC, GN and PbO/GN/AC composite between -0.85 V and -1.50 V at a scan rate of $1 \text{ mV} \cdot \text{s}^{-1}$. As can be seen from the figure, the polarization curve of GN does not attain apparent stabilization stage. When the potential reaches to -1.05 V , the polarization curves of AC and PbO/GN/AC composite tend to approach stabilization, and the systems are close to equilibrium state. At -1.15 V , the reaction of hydrogen evolution increases gradually with the increase of polarization current. Meanwhile, the hydrogen-evolution currents of GN and AC increase rapidly, while that of PbO/GN/AC composite quite gently. The probable

reason was that Pb element has the higher overpotential of hydrogen evolution, which affects the activity of hydrogen evolution on the surface of the AC or graphene and increases the difficulty of the hydrogen evolution, therefore, the hydrogen evolution of the AC or GN was diminished.

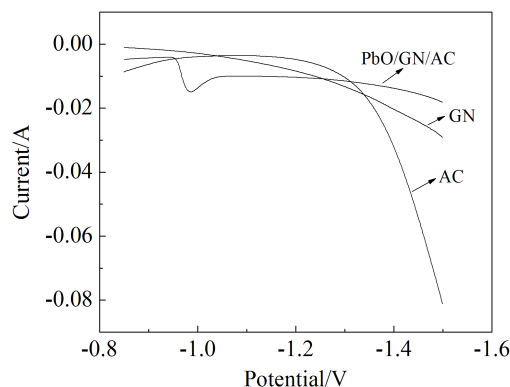


Fig. 4 Linear sweep voltammograms of GN, AC and PbO/GN/AC composite electrodes

A comparison in CV curves of AC, GN and PbO/GN/AC composite electrodes at $10 \text{ mV} \cdot \text{s}^{-1}$ is shown in Fig. 5A. For the composite, the double layer capacitance plays an important role at the beginning. A pair of obvious redox peaks of lead is observed in the potential range between -0.85 and -1.1 V . As can be seen from Fig. 5A, the capacitance of composite has a significant improvement compared with those of both purified AC and GN. The electric double layer capacitance of the carbon electrode remains largely unaffected by the immobilization of the redox couple of Pb/PbSO₄. At the beginning, the capacitor performance is from the embodiment of the double layer. As the potential reaches a certain value, which is the potential for the electrochemical redox reaction to take place, the double layer capacitance decreases. This observation can be related with the concomitant loss of macroporosity and mesoporosity surface area. Thus, the redox reaction occurred in the surface of macroporosity and mesoporosity of the carbon progressively hinders the efficiently access of electrolyte ions to the smallest pores. Evidently, these pores do not significantly contribute to the double layer capacitance in H₂SO₄ electrolyte. As the reaction occurs,

the extent of the redox reaction increases gradually, which leads to a redox couple providing pseudocapacitance in a composite electrode. The partial loss of the EDLC is balanced with the redox capacitance of lead. Thus, the overall capacitance of the composite electrode is the sum of the EDL capacitance and the redox capacitance. As for the AC and GN, their capacitances are only from the double layers. The addition of graphene additives promotes the actions of two kinds of capacitors. In addition, a distinct inflection point of hydrogen evolution turns up on AC electrode at about -1.15 V and graphene has none. However, the ternary composite has the higher overpotential of the hydrogen reaction. Fig. 5B shows the CV curves of the PbO/GN/AC composite electrodes at different potential scan rates of $5, 10, 20, 50, 100$ and $200 \text{ mV} \cdot \text{s}^{-1}$. The current gradually deviates from zero line of current and the extent of excursion amplifies as the scanning rate increases. Furthermore, when the scanning rate is larger than $100 \text{ mV} \cdot \text{s}^{-1}$, the reduction process of lead is difficult to conduct fully. This may be that hydrogen ions in the electrolyte can not timely migrate and diffuse to the surface of active mass. On the other hand, significant amounts of PbSO₄ crystal in the active mass cannot completely dissolved. However, the increasing trend of cathode current of hydrogen evolution is basically identical at different scan rates, which implies that the PbO/GN/AC composite can suppress the stability of the hydrogen evolution and can resist large current shock during the cathodic run completely.

Charge-discharge measurements are critical in the analysis and prediction of the active materials performance under practical operating conditions. To accurately determine the electrochemical behavior of the novel supercapacitors, the galvanostatic charge-discharge performances of AC, GN and PbO/GN/AC composite as electrodes were tested at varying currents. The average specific capacitance (C_{spec}) of all the porous electrodes in supercapacitor is calculated as:

$$C_{\text{spec}} = \frac{i_0 \Delta t}{m \Delta V} \quad (1)$$

where i_0 is the constant charge/discharge current (A), Δt is the discharge time (s), ΔV is the potential

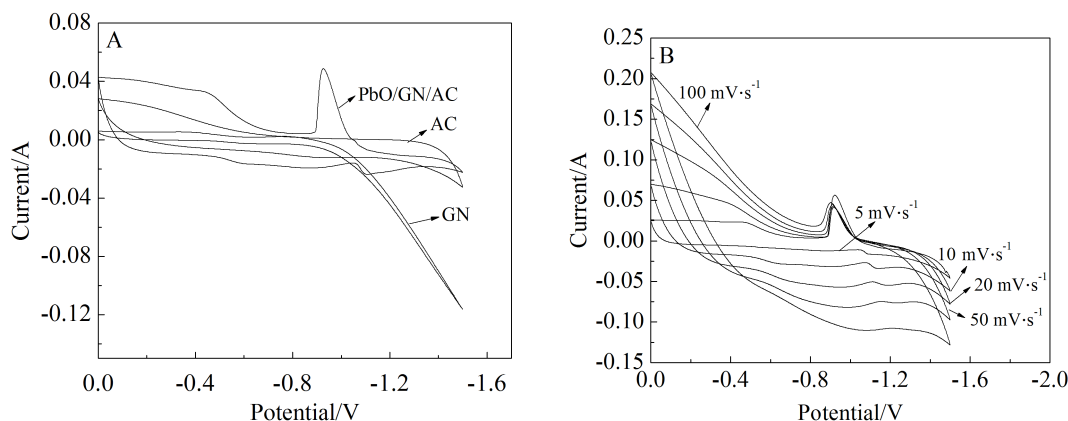


Fig. 5 A. Cyclic voltammograms of GN, AC, and PbO/GN/AC composite electrodes at scanning rate of 10 mV·s⁻¹; B. cyclic voltammograms of PbO/GN/AC composite electrodes with various scan rates

difference (V) during the discharge process, and m is the mass of active material of the electrodes (g).

Fig. 6A shows the galvanostatic charge/discharge curves of AC, GN and PbO/GN/AC composite electrodes at a constant current of 10 mA in the potential range between -1.0 V and 0.0 V. From these curves, the specific capacitance of the PbO/GN/AC composite electrode is calculated to be 312.6 F·g⁻¹, twice as high as that of the pure AC electrode (168.6 F·g⁻¹). For GN based supercapacitor, the specific capacitance is 133 F·g⁻¹. Surprisingly, introduction of lead does not affect the capacitance of the composite. It is believed that the good specific capacitance of composite electrodes is mainly due to the increased surface area and consistently high electrical conductivity. The smaller particles have less effect on the

pore structure of activated carbon. The existence of Pb results in redox processes occurring at or near the electrode surface, which can provide the pseudocapacitance and enhance the charge storage capability. Furthermore, the wrinkle and an open pore system formed by GN not only facilitate the access of the electrolyte ions onto the AC surface, but also improve the interaction between PbO particles and AC, making electron transport easier between AC and PbO. Additionally, the high specific capacitance value confirms that the combination of all three types of the materials allows maximizing the utilization of AC. Obviously, large internal resistance and contact resistance between the AC exist, as evident by a noticeable IR drop in the discharge curve in the AC electrode as shown in Fig. 7. However, the IR drop of the

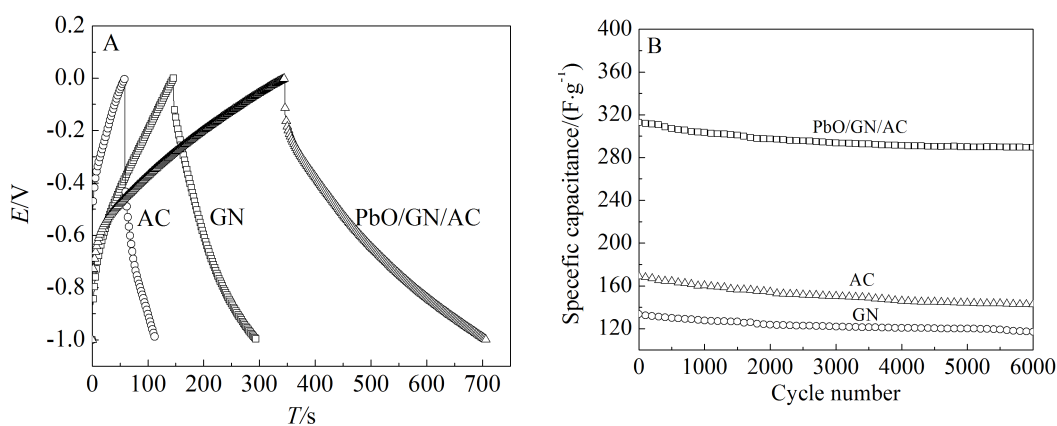


Fig. 6 Galvanostatic charge/discharge curves (A) and the specific capacitance change as a function of cycle number for GN, AC and PbO/GN/AC composite electrodes at 10 mA·cm⁻² (B)

composite is significantly lower than that of the AC electrode. These results indicate that the unique inter-layering graphene nanosheets effectively suppress the internal electrical resistance of the electrodes.

For practical applications, electrochemical stability is one of the crucial factors to supercapacitors^[11]. The cycling life test of the supercapacitor devices is evaluated by conducting galvanostatic charge-discharge measurements for 6000 cycles at a constant current of 10 mA in the potential range between 0.0 V and -1.0 V. The specific capacitance as a function of cycle number is presented in Fig. 6B. The AC, GN and PbO/GN/AC based supercapacitors are found to exhibit excellent cycle life over the entire cycle numbers. It is noteworthy that the specific capacitance of the composite electrode still remains a high value of $289.5 \text{ F} \cdot \text{g}^{-1}$ ($\sim 92.6\%$) after 6000 cycles. This illustrates that the PbO/GN/AC based supercapacitor possesses good stability, lifetime and a very high degree of reversibility in the repetitive charge-discharge cycling. Charge-discharge cycle test of the ternary composite film suggests that the synergetic interaction among AC, GN, and PbO significantly improves the electrical properties and the mechanical stability of the electrode.

To further investigate the electrochemical performance of the capacitors, electrochemical impedance spectroscopy (EIS) was employed. The EIS data were recorded under the frequency range from 0.01 Hz to 100 kHz. The Nyquist plots of the AC, GN and PbO/GN/AC composite electrodes are shown in Fig. 7. Plots show a semicircle in the high frequency region and a straight line in the low frequency region. In the range of high frequency, the intercept of the semicircle with the real axis represents equivalent series resistance (ESR), including the resistance of the electrolyte solution, the intrinsic resistance of activation material, and the contact resistance of the interface active material current collector. The slope of the 45° portion of the curve is called the Warburg resistance and is a result of the frequency dependence of ion diffusion in the electrolyte to the electrode interface^[12]. The vertical line at lower frequencies parallel to the imaginary axis indicates an ideal behavior, representative of the ion diffusion in the structure of

the electrode. It has been shown that the internal resistances of the GN, AC and PbO/GN/AC composite electrodes are 2.26Ω , 2.60Ω and 1.56Ω , respectively. These results imply that the graphene nanosheets suppress the electrode resistance, corresponding to a smaller IR drop as observed in Fig. 6A. Additionally, the reduction in the ESR value for the PbO/GN/AC composite indicates that AC and PbO provide diffusion path between sheets and improve charge transfer performance of GN.

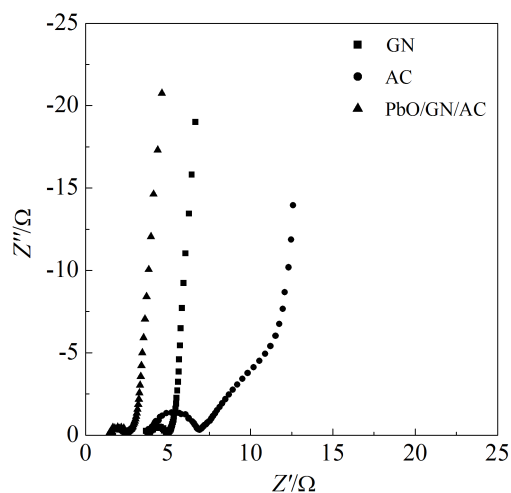


Fig. 7 Nyquist plots for pure GN, AC and PbO/GN/AC composite electrodes

Cycling lives of ultra-battery and conventional lead-acid batteries under simplified pattern are shown in Fig. 8. The cycle life of the lead-acid batteries is less than 4200 cycles, while that of the ultra-battery up to 18000 cycles, approximately 3.5 times longer than that of the lead-acid batteries. The results indicate that the PbO/GN/AC composite has a positive effect on lead-acid batteries.

3 Conclusions

In summary, a simple approach is developed successfully to synthesize PbO/GN/AC composite. The additions of AC and PbO into graphene layers aim to improve electrolyte-electrode accessibility and the capacitance properties of GN by reducing the agglomeration of GN. The presence of GN monolayer provides an electronically conducting pathway through PbSO_4 regions, large surface area for dispersing lead sulfate particles and storing electrolyte ions

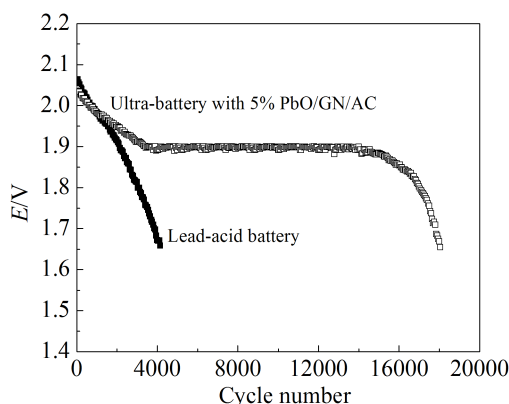


Fig. 8 Cycling performances of ultra-battery and conventional lead-acid batteries under simplified pattern

to speed up mass transfer. Electrochemical measurements indicate that the composite possesses the higher over-potential of hydrogen evolution, high specific capacitance and good affinity of the carbon additive to lead. By adding 5% (by mass) of PbO/GN/AC to the negative paste, the ultra-battery shows a superior cycle life to the conventional lead-acid battery. These features make PbO/GN/AC composite quite a suitable and promising material for lead-acid battery.

References:

- [1] Czerwinski A, Obrebowski S, Kotowski J, et al. Hybrid lead-acid battery with reticulated vitreous carbon as a carrier- and current-collector of negative plate[J]. Journal of Power Sources, 2010, 195(2): 7530-7534.
- [2] Lam L T, R Louey. Development of ultra-battery for hybrid-electric vehicle applications[J]. Journal of Power Sources, 2006, 158(2): 1140-1148.
- [3] Lam L T, Louey R, Haigh N P, et al. VRLA ultrabattery for high rate partial state of charge operation[J]. Journal of Power Sources, 2007, 174(1): 16-29.
- [4] Cooper A, Furakawa J, Lam L, et al. The ultrabattery-A new battery design for a new beginning in hybrid electric vehicle energy storage[J]. Journal of Power Sources, 2009, 188(2): 642-649.
- [5] Furukawa J, Takada T, Monma D, et al. Further demonstration of the VRLA-type ultrabattery under medium-HEV duty and development of the flooded-type Ultra-Battery for micro- HEV applications[J]. Journal of Power Sources, 2010, 195(4): 1241-1245.
- [6] Aravinda L S, Bhat, K U, Bhat B R. Nano CeO₂/activated carbon based composite electrodes for high performance supercapacitor[J]. Materials Letters, 2013, 112(1): 158-161.
- [7] Feng Z H, Xue R S, Shao X H. Highly mesoporous carbonaceous material of activated carbon beads for electric double layer capacitor[J]. Electrochimica Acta, 2010, 55 (24): 7334-7340.
- [8] Geim A K. Graphene: Status and prospects[J]. Science, 2009, 324(5934): 1530-1534.
- [9] Katsnelson M I. Graphene: Carbon in two dimensions[J]. Materials Today, 2007, 10(1/2): 20-27.
- [10] Novoselov K S. Nobel Lecture: Graphene: Materials in the Flatland[J]. Reviews of Modern Physics, 2011, 83(3): 837-849.
- [11] Hou Y, Cheng Y W, Hobson T. Design and synthesis of hierarchical MnO₂ nanospheres/carbon nanotubes/conducting polymer ternary composite for high performance electrochemical electrodes[J]. Nano Letters, 2010, 10(7): 2727-2733.
- [12] Qu D Y, Shi H. Studies of the activated carbons used in double-layer supercapacitors[J]. Journal of Power Sources, 2002, 109(2): 403-411.

氧化铅/石墨烯/活性炭的制备及电化学行为

高云芳*, 王艳平, 姚秋实, 王福华, 任冬雷, 徐 新

(浙江工业大学 化学工程学院, 绿色化学合成技术国家重点实验室培育基地, 浙江 杭州 310032)

摘要: 将商业活性炭和石墨烯在饱和硝酸铅溶液中超声浸渍, 并通过化学沉积结合高温煅烧制备了氧化铅/石墨烯/活性炭(PbO/GN/AC)复合材料. 采用 XRD、SEM、EDS 等手段对复合物进行了物相及微观结构表征. 测试结果表明, 直径约 200 nm 的 PbO 颗粒均匀地分散在活性炭和石墨烯的表面. 复合物表现出优异的电化学性能, 具有较高的析氢过电位, 比电容高达 312.6 F·g⁻¹, 等效串联内阻仅为 1.56 Ω. 6000 次循环之后, 复合物电极的电容保持率仍达到 92.6%. 将 5% (by mass) 的 Pb(PbO)/ 活性炭材料加入到铅酸电池负极铅膏中制备相应铅炭超级电池, 循环次数达到 18051 次, 是普通铅酸蓄电池的 3.5 倍.

关键词: 活性炭; PbO; 石墨烯; 析氢; 超级电容器